Postbuckling Analyses of Elastic Cylindrical Shells under Axial Compression

Takaya Kobayashi and Yasuko Mihara

Mechanical Design & Analysis Corporation
Tokyo, Japan

Abstract: In the design of a modern lightweight structure, it is of technical importance to assure its safety against the buckling under the applied loading conditions. For this issue, the determination of the critical load in an ideal condition is not sufficient, but it is further required to clarify the postbuckling behavior, that is, the behavior of the structure after passing through the critical load. One of the reasons is to estimate the effect of practically unavoidable imperfections on the critical load and the second is to evaluate the ultimate strength to exploit the load-carrying capacity of the structure. For the buckling problem of circular cylindrical shells under axial compression, a number of experimental and theoretical studies have been made by many researchers. In the case of the very thin shell that exhibits elastic buckling, experimental results show that after the primary buckling, secondary buckling takes place accompanying successive reductions in the number of the circumferential waves at every mode shift on one-by-one step. In this paper we traced this successive buckling of circular cylindrical shells using the latest in general-purpose FEM technology. We carried out our studies with three approaches; one is to use the arc-length method (the modified Riks method), the second is static stabilizing with the aid of (artificial) damping especially for the local instability and the third is to use the explicit dynamic procedure. The studies accomplished the simulation of the successive buckling following unstable paths, and show good agreement with the experimental results.

Key words: Shell, Buckling, Riks method, Artificial damping, Explicit dynamic.

1. Introduction

Modern structures are designed, for the most part, as those that are assembled with the combined use of thin shells and slender members to fulfill the contradictory requirements of reduced weight and high strength. This type of member typically has a small ratio of thickness/cross-sectional area relative to its overall structural dimensions. If used simply in a state where it is subjected to tensile stresses, such a member will maintain an adequate level of strength. However, if the same member is used in a state where it is subjected to compressive or shear stresses, it will be unable to keep stable equilibrium when its deflection or applied force exceeds a certain critical value, at which the current form of stable equilibrium may transition to another state of equilibrium or the member will suddenly deform to collapse. Such a phenomenon is called elastic stability or more commonly buckling. The term “postbuckling” refers to the behavior of a structure exhibited after passing beyond a certain critical values of elastic stability. As a typical example, let us consider the case of a bar column or a rectangular plate subjected to a compressive load as shown in Fig.1. In this figure, P_{cr} indicates the point at which the critical load is met. The area before P_{cr} is the non-buckled region and the area after it is the buckled region. Up to P_{cr}, the load increases almost linearly, regardless of the structure's shape, but after crossing P_{cr}, the structures behave in a very different manner, depending on their respective shape.

In the column's case, after the column buckles due to simple compression, the deflected profile shifts to a bent form. This problem is called elastica, and its most striking characteristic is an extremely high lateral deflection due to bending compared to compressive deformation. Consequently, the postbuckled load remains almost unchanged from P_{cr}. Since the lateral displacement produced is so large, any initial warp (e.g., initial imperfection), if it exists at all, will not greatly affect the column's behavior. The load-displacement curve indicated by dotted lines in Fig.1 shows the behavior when there is some initial imperfection. Although the point at which buckling begins will be unclear due to such initial imperfections, we can see that ultimately the magnitude of the load is asymptotic to P_{cr}.

In the rectangular plate's case, its behavior when simply supported along its transverse edges and compressed in the axial direction is well known. In this case, sinusoidal out-of-plane deformations occur not only along the axial direction, but also widthwise, causing the center of the plate to bulge. According to the concept of finite displacement, the simply supported edges escape out-of-plane deflection due to the bulging at the center of the plate. Consequently, the deformed pattern of the plate can sustain a larger compressive load than that carried by the simply axial-bent form of the column. That is to say, the load continues to increase gradually even after exceeding P_{cr}, and thus the plate will not readily collapse, even though the column will do so. In addition, this deformation pattern will be insensitive to any initial imperfection. Many assembled structures take advantage of this capability of shell plates (known as the theory of the effective width) to increase their ultimate strength after crossing the buckling point.

To utilize the postbuckling analysis is an efficient way to find the ultimate strength in the final stage of deformed structures as well as for evaluating the effect due to initial imperfections. This study covers the case of a cylindrical shell structure that exhibits unique behavior largely different from those of a column or plate. This paper will present the findings from our attempt to derive solutions on the postbuckling strength for this cylindrical shell using the latest in general-purpose FEM technology. Elastic buckling of cylindrical shells under axial compression is regarded as a fundamental issue in the buckling of shell structures. It is probably fair to say that the foundations of shell stability theory were almost all laid in the study of this subject [1]. In the field of actual products, the application of this buckling problem has been widened, beginning with the design of aircraft fuselages or liquid storage tanks and extending to cover new fields, such as impact energy absorption mechanisms. The classic theoretical solution to critical buckling stress can be expressed as in Eq. 1, which was derived already in 1910s.

Classical elastic critical stress :
$$\sigma_{cl} = \frac{E}{\sqrt{3\left(1-\nu^2\right)}}\frac{t}{r} \simeq 0.605E\frac{t}{r} \quad \cdots (1)$$

where, E: Young's modulus ν: Poisson's ratio r: cylinder radius t: shell wall thickness

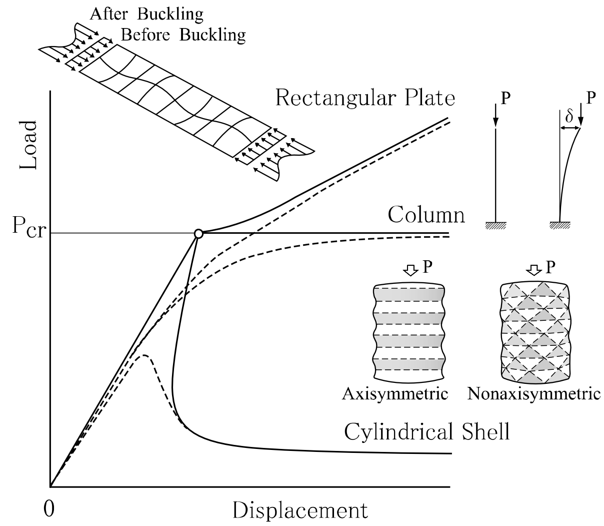

Figure 1. Load-displacement curves for postbuckling of a bar, rectangular plate and cylindrical shell.

Eq. 1 was originally derived using the energy method in which axisymmetric waves were assumed to form along the entire length of the cylinder (i.e. a corrugated appearance with waves only in the axial direction). However, it should be noted that the axisymmetric deformation as assumed here can be substantiated only if the circumferential length of the cylinder varies as the deformation progresses. The form of buckling accompanied by changes in the length of the member is known as "extensional buckling". P_{cr} for cylindrical shells indicated in Fig.1 is the critical load corresponding to this extensional buckling. As can be easily surmised, such extensional deformation requires a lot of strain energy, and is likely to shift to a non-extensional deformation for which a much lower level of energy is adequate.

According to the modern stability theory, the classical result Eq.1 also gives the critical stress with a mode shape that is sinusoidal both axially and circumferentially. At this critical stress, a very large number of different buckling modes or eigenmodes are all simultaneously critical (sometimes over 100 modes with loads within 1%) [1]. Many modes are possible in different asymmetric patterns (Fig.1) whose wavelengths in the axial and circumferential directions are related by the 'Koiter circle' [2], [3]. The asymmetric buckling pattern, the so-called diamond buckling pattern, can be characterized by ridges in two inclined directions and furrows in circumferential directions. A typical asymmetric buckling pattern observed in experiments will be shown in Fig.3 in the following section. The combined length of all the furrows in each cross section is approximately equal to the length of the original circle. Therefore a non-extensional deformation is achieved, and the cylindrical shell tends to have the asymmetric buckling pattern. Consequently, even if a cylindrical shell reaches classic axisymmetric buckling, deformation will progress to the next stage of instability at which the load will be dramatically decreased. The steeply falling unstable postbuckling path in Fig.1 is associated with the proximity of the above-mentioned many asymmetric modes, while the classical axisymmetric mode has a stable postbuckling path and is later found to be important when the cylinder is internally pressurized [1].

Axially compressed cylindrical shells are known to be the most imperfection sensitive among known cases, matched only by complete spherical shells under external pressure. If a cylindrical shell has a perfect geometry, it will deform axisymmetrically and bear up to the classic critical load. However, if the cylinder has some initial imperfections, such as circumferential deviations from an ideal circular shape or deviations in shell thickness over the surface, such imperfections will serve as a trigger that will produce waves in the circumferential direction, and accordingly, the deformed shape will readily become non-axisymmetrical. The finding as mentioned in the above may be summarized as follows:

- The classical elastic critical stress can give the critical load of axisymmetric buckling, but, there are simultaneously many bifurcation points in the vicinity of the critical load where the deformation path begins to turn towards axially asymmetric buckling.
- Accordingly, even though the initial deformation pattern of the cylindrical shell is axisymmetric mode, the successive deformed forms shift to axially asymmetric mode soon after occurrence of buckling. At the same time the load suddenly decreases because of that the load carrying capacity of the axially asymmetric mode is much less than that of the axisymmetric mode.
- Transition to this axially asymmetric mode is excited by slight imperfection which inherently exists in any real shell structure. Particularly for a case of thin shell structures, the axially asymmetric buckling will usually take place under the much smaller stress before reaching the classical elastic critical stress. Because such imperfection causes not only deformation patterns led to bifurcation paths, but also decreasing of bifurcation stresses themselves (strictly speaking, the bifurcation point is changed to the limit point, as described later).
- Consequently, the buckling stresses observed in the actual measurement are found to be not only lower than those theoretically estimated, but also in widely scattered distribution. It is empirically known that the actual measurement results are only 10-60% of the theoretically predicted values.
- Many bifurcation paths leading to axially asymmetric buckling mode exist in the very narrow range on the load-displacement plane. Therefore, the imperfection may affect which bifurcation path the deformation path is led. Since the load bearing capacity of shell structures depends on deformation modes, the initial imperfection influences not only simply the initial buckling behavior but also the ultimate strength of the structure.
- Especially, if plasticity occurs intermediately along the deformation path, the deformation mode remains at that stage with no sign of any transition. Accordingly it should be noted that some specific deformation modes are likely to be selectively progressed keeping the affect by the initial imperfection.

2. Findings from Previous Research on Postbuckling Behavior

It was not until the 1950s that it was fully understood that the interaction between unavoidable imperfections and the ill-natured postbuckling behavior was the reason for the large discrepancies between observed buckling loads and the predictions of the classical theory. The most important contributions to the development of this understanding were those of Karman and Tsien [4] and Donnell and Wan [5] who firstly calculated complete load-displacement curves of axially compressed cylinders with perfect and imperfect geometry, respectively, using nonlinear large-displacement formulations of Donnell's shell theory. They showed that a buckled shell in the deep postcritical range can be in equilibrium under a load much smaller than the classical buckling load predicted by a small-deflection theory. Fig.2 shows an example of the load-displacement curve given by Karman and Tsien [4]. They assumed the form of postbuckled cylindrical shells in which m and n are parameters defining the number of waves in the axial and circumferential direction respectively. In this figure, the compressive displacement rendered dimensionless by shell thickness is the abscissa, and the critical stress rendered dimensionless by the radius is the ordinate. All curves in this figure indicate the results with the number of circumferential waves n as a parameter. As seen in the figure, all the curves are concave, and as the value of n decreases, the minimum value shifts to the right. By drawing an envelope passing these minimal values, we find that the left end of the figure, i.e., the value of y-intercepted, takes a value of 0.605 in the case of ν=0.3, as shown below. This value coincides with the classical elastic critical stress given by Eq. 1.

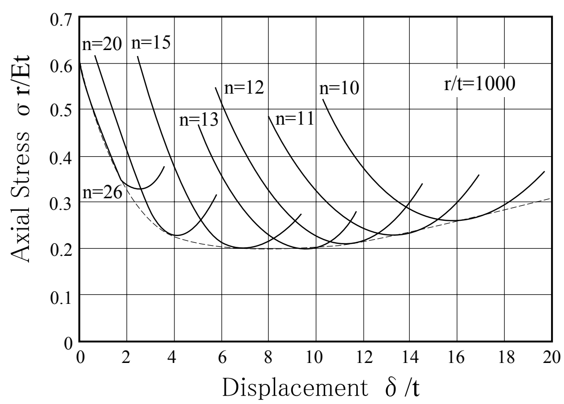

The y-intercept by the envelop of the minimal values :

$$\left(\frac{\sigma r}{Et}\right)_{min} = \frac{1}{\sqrt{3\left(1-\nu^2\right)}} = 0.605$$

Figure 2. Load-displacement curves with different number of circumferential waves, Karman and Tsien [4].

Based on Fig.2, the following scenario for the buckling process is assumed to be taken.

(1) When a cylinder is subjected to axial compression, it holds the load bearing capacity continuously sustaining the compressive stresses lower than the classical elastic critical stress under which theoretically axisymmetric buckling takes place.

(2) In the postbuckling region, the deformation mode is bifurcated towards the axially asymmetric deformation mode. The curves shown in Fig. 2 correspond to the postbuckling path after meeting the bifurcation point. For the case in Fig. 2, the axially asymmetric mode with the number of circumferential waves of n=26 should first occur. As mentioned previously, if the amplitude of initial imperfection is large, this type of axially asymmetric buckling may occur bypassing the axisymmetric buckling.

(3) In accordance with the progress of deformations, the load continues to decrease until reaching

the minimal value and then begins to increase. However, another buckling curve with a lesser number of waves exists adjacently on the right of the Fig.2, and since it requires smaller loads to produce the same deflection than the current curve does, the current deformed pattern transitions to the next curve in snap-through manner.

(4) The above steps are repeated in a sequence of deformation transition.

That is to say, Fig.2 suggests the possible occurrence of a characteristic phenomenon such that the deformed pattern of a cylinder under axial compression progresses discontinuously, repeating snap-through to the next mode with a lesser number of waves.

There are systematic findings obtained by a group led by Yamaki et al. for the elastic buckling of cylindrical shells (not limited to the case of axial compression). The product of their experiments and theoretical approaches are covered with literature [6] in Reference list, and their achievement is still rated as one of the most reliable results to date. Fig.3 shows their typical results. All the cylinder models were constructed from polyester film and finished with the careful cleanup of geometric imperfections. Each model was fully fixed at both ends, and then compressed in the axial direction. The test models provided are those with the same diameter but different heights from each other. A shape parameter (Batdorf parameter) Z is defined as follows,

Batdorf parameter : $$Z = \sqrt{1-\nu^2}\,\frac{L^2}{rt} \qquad \cdots (2)$$

Fig.3(b) shows the load-displacement curves obtained by their experiment for the test cylinder with Z=500. As discussed above, after the primary buckling occurred under the classic critical load P_{cr}, the deformed pattern of a cylinder progresses discontinuously while the number of waves in the circumferential direction decreases. The number of circumferential waves is found to be first n=12, and subsequently observed up to n=9 in the figure. The pioneering research work done by Karman et al., as shown in Fig. 2, can be evaluated as such that their finding precisely points out the intrinsic nature of such the postbuckling path observed in this experiment.

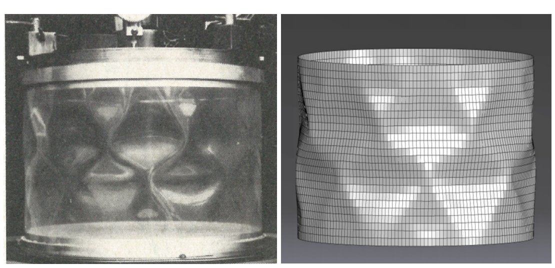

Experiment (Yamaki) FEM (This study)

Z=500 (r=100mm, t=0.247mm, L=113.9mm)

E=5560 MPa, ν=0.3

(a) Deformation of test cylindrical shell (δ =0.606mm)

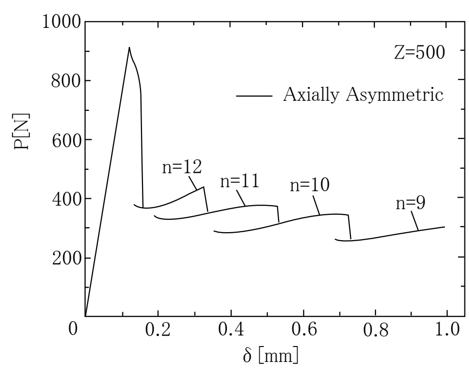

(b) Load-displacement curves

Figure 3. Experimental results by Yamaki et al. [6].

The numerical analysis done by Teng and Hong [7], [8] is one of the most successful results among recent research works. They analyzed the postbuckling taking initial imperfection into account of a rotating shell structure modeled with axisymmetric shell elements using the semi-analytical method with the circumferential variables approximated by the Fourier series. Fig.4(a) shows different paths of postbuckling obtained from the model subjected to the initial imperfection defined in terms of eigenmodes having different number of waves in circumferential direction. For example, let's consider the path for n=16. After passing the primary buckling point, A, the displacement is reversed and the load is lowered to reach the minimal value, B. The path from A to B represents a simultaneous process transforming the membrane compression energy to bending energy. Since the deflection associated with bending deformation is substantially larger than the deflection associated with membrane compression, the reduction of end displacements of the cylindrical shell is accompanied by a large accumulation of radial displacements. After the minimal value, B, the load increases to reach the maximum value at the second buckling point, C. Then the path again loses its stability with reversing of displacements.

The most excellent mark in their research work is such that the point of the second buckling (point, C) was precisely identified. The more the number of circumferential waves, n, decreases, the more appearance of the second buckling point delays and the load is lowered along the path. In accordance with the bifurcation theory by Fujii, Noguchi and Ramm [9], the above-mentioned primary buckling point, A is distinguished as bifurcation point, and the minimal value, B as limit point, and the secondary buckling point also as limit point. The path A-B is an unstable path on which the stiffness matrix becomes non-positive definite. The path B-C is a stable path along which its stiffness matrix keeps positive definite. These postbuckling curves were examined using the arc-length method, and accordingly the unstable region on the path A-B where the displacement is reversed can be obtained. However, the displacement will increases monotonously in the actual loading process, the reverse of displacement will not be observed but snap-through behavior will be observed instead. Fujii et al. pointed out that such a type of jump takes place towards the stable path on which the load is lowered and the slope is positive (the stiffness matrix is positive definite).

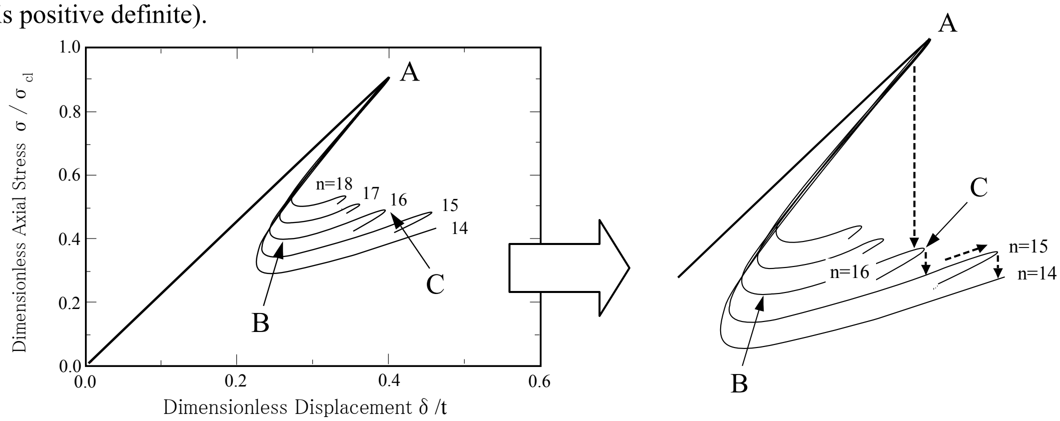

(a) Postbuckling paths of various harmonic modes (b) Estimated mode jumping for actual behavior

Figure 4. Numerical result by Teng and Hong [7] and its interpretation based on findings from Fujii, Noguchi and Ramm [9].

Fig.4(b) magnifies a portion of Fig.4(a). According to Fujii's finding, deformation process can be predicted in such a way that the deformation, after passing the primary buckling point, A, jumps to the path of n=16, followed by jumping to the path of n=15, subsequently to the path of n=14 in this sequence. A dotted line in Fig.4(b) indicates the predicted path. The results obtained from the experiments by Yamaki et al., as illustrated in Fig.3(b), fully support the hypothesis as described above.

3. Postbuckling Analysis Using General-Purpose FEM

According to the recent enhancement on the computers, even an analysis of a 3D shell structure is regarded as just a daily routine work. Along with this, a new trend is on going such that the stability analysis of shell structures with very advanced and sophisticated approaches are being attempted to switch to the analysis using some general-purpose FEM codes instead. As typical case, Croll and his group [10] reports the case with the use of a general purpose FEM code in lieu of using the reduced-stiffness method that has ever contributed for obtaining remarkable achievement. Now we proceed with the study to reproduce the Yamaki's experimental results employing Abaqus [11].

3.1 Practical Postbuckling Analysis and Imperfections

The difference between the respective load-carrying capacity of a shell structure with ideally accurate dimensions of its geometry and a real structure actually assembled is one of the most important tasks for the designers to exactly figure out. Such the difference may be caused by that shell structures inevitably hold high imperfection sensitivity. As mentioned previously, it is a critical point that the buckling loads observed in experiments always found to be not only much lower than those derived from the classical theories, but also in widely scattered distribution. Besides these buckling loads, involvement of the difficulty with predicting their buckling modes makes the problem further complicated. Typically, the European standard for steel shell structures [12] regulates that, when geometric nonlinear analysis is applied for the structures with explicit representation of initial imperfection, and if any specific pattern of the imperfection holding high risk of structural damages is not able to be identified, a possible range including risky imperfection dimensions should be explored. The code also recommends such that the imperfection should be specified in terms of the buckling modes, obtained from linear elastic bifurcation analysis, unless undesirable imperfection geometry can not be identified individually. It should be noted that the buckling modes resulted from the linear elastic bifurcation analysis do not make sure that they are consistent with the buckling modes occur in real cases [13]. For remarks on conducting the actual design, refer to the guidance found in literature by Rotter [1].

From the above-mentioned point of view, this study mainly aimed to prove that the analysis for the cylindrical shell structure with perfect geometry can be performed through the region extending to deep postbuckling range using the general purpose FEM code. Due to some restraints imposed on the analysis, a linear buckling mode was employed as the initial imperfection so that it may trigger steering deformation patterns to bifurcation path. But we recognize it as such a way that is adopted simply as an analytic tactics. Fig. 5 shows the relation between the buckling stress and the amplitude of imperfection, which was organized by Rotter [1]. When the amplitude of imperfection is about 0.01 of the shell thickness, the buckling response of the cylindrical shell under axial compression is estimated as being so close to the result obtainable from the shell with perfect geometry. The linear buckling modes were so scaled that they can be mapped on the initial perfect geometry in order to generate perturbed mesh. The range of perturbation as 0.01 times the shell thickness was used in this study.

3.2 Analyzing Unstable Response: 1. Arc-length Method

Geometrically nonlinear static problems sometimes involve buckling or collapse behavior, where the load-displacement response shows a negative stiffness and the structure must release strain energy to remain in equilibrium. Several approaches are possible for modeling such behavior. Among them, path-tracing based upon arc-length method (modified Riks method in Abaqus) is the most fundamental procedure to study the postbuckling behavior of shell structures. This method is used for cases where the loading is proportional; that is, where the load magnitudes are governed by a single scalar parameter. Therefore, this method is not applicable to problems subject to multiple loads acting independently. The arc-length method works well in snap-through problems—those in which the equilibrium path in load-displacement space is smooth and does not branch. Generally you do not need take any special precautions in problems that do not exhibit branching (bifurcation). The arc-length method can also be used to solve postbuckling problems with bifurcation. However, the exact branch-switching problem cannot be analyzed directly due to the discontinuous response at the bifurcation point. To analyze a branch-switching problem, it must be turned into a problem with continuous response instead of bifurcation. This effect can be accomplished by introducing an initial imperfection into a perfect geometry so that there is some response in the buckling mode before the critical load is reached. From the buckling theory aspect, this operation is equivalent to converting the bifurcation point to the limit point, as shown in Fig.6. That is, the path after bifurcation which is naturally the secondary path is changed to a smooth primary path. Imperfections are usually formed with perturbations in the geometry of structures. Imperfection represented with a linear buckling mode can be advantageously applied to the practical analysis as described in the above.

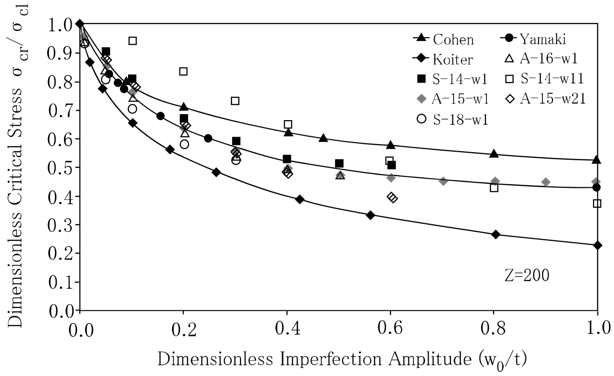

Figure 5. Sensitivity of bifurcation load to amplitude of asymmetric imperfections, Rotter [1].

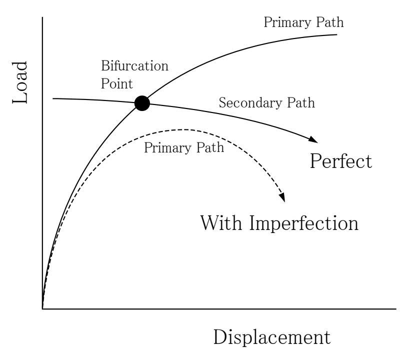

Figure 6. Smoothing bifurcation discontinuity by introducing imperfections.

3.3 Analyzing Unstable Response: 2. Artificial Damping Method

The arc-length method realizes the stable analysis process under the global load control. If the analysis process traces unstable paths under the global load-displacement response with negative stiffness, the arc-length method is effectively usable. However, if the instability is localized (e.g., surface wrinkling, material instability, or local buckling), there will be a local transfer of strain energy from one part of the model to neighboring parts, and global solution methods may not work. This class of problems has to be solved either dynamically or with the aid of (artificial) damping; for example, by using dashpots. Buckling of a real, thin-walled shell is typically a very local phenomenon, which may be triggered by a small, local disturbance. It has for instance been observed by high-speed photography, that when an isotropic cylindrical shell is compressed axially, single relatively small almost quadratic buckles form at the beginning of the buckling process. The size of these buckles may be characterized as $4\sqrt{\mathrm{rt}}$. This value has been chosen as gauge length when measuring initial imperfection amplitude [1], [14]. Abaqus provides an automatic mechanism for stabilizing unstable quasi-static problems through the automatic addition of volume-proportional damping to the model. Viscous forces of the form $\mathbf{F}_\mathrm{V} = \mathrm{c}\mathbf{M}^*\mathbf{v}$ are added to the global equilibrium equations $\mathbf{P} - \mathbf{I} - \mathbf{F}_\mathrm{V} = 0$. Where $\mathbf{M}^*$ is an artificial mass matrix calculated with unity density, *c* is a damping factor, $\mathbf{v} = \Delta\mathbf{u} / \Delta\mathrm{t}$ is the vector of nodal velocities, $\Delta\mathrm{t}$ is the increment of time (which may or may not have a physical meaning in the context of the problem being solved), $\mathbf{P}$ is the total applied load, and $\mathbf{I}$ is the structure's internal force. When local instability occurs, the deformation rate of that portion begins to increase, and consequently, locally released strain energy is dissipated due to the appended damping effect. The ratio of the dissipated energy to the strain energy is called the energy ratio (Dissipated Energy Fraction), and it has a default value of 2.0E-04 in Abaqus. The damping coefficient should be appropriate for the purpose (i.e., not too large), the damping coefficient applied in our analysis was lowered to 1/1000 of the default.

3.4 Analyzing Unstable Response: 3. Explicit Dynamic Analysis

This nonlinear equation solving process is expensive; and if the equations are very nonlinear, it may be difficult to obtain a solution. However, nonlinearities are usually more simply accounted for in dynamic situations than in static situations because the inertia terms provide stability to the system; thus, the method is successful in all but the most extreme cases. Especially the explicit integration method is more efficient than the implicit integration method for solving extremely discontinuous events or processes. The explicit dynamics procedure performs a large number of small time increments efficiently. An explicit central-difference time integration rule is used; each increment is relatively inexpensive because there is no solution for a set of simultaneous equations. Many of the advantages of the explicit procedure also apply to slower (quasi-static) processes. The postbuckling behavior of axially compressed cylindrical shells may be represented by dynamic mode jumping. From the view point of the history in the traditional research work, it is reasonable for us to consider that the essential nature of postbuckling behavior can be regarded as a static problem, even though it may possible to rise some side issues such as occurrence of overshooting in deformation due to the inertia effect. In this study, the explicit dynamic analysis method was applied. However, the reason to do so is simply relying on the toughness of the analysis process, but is not to aim to conduct the simulation for the dynamic effect. A sufficiently slow axial velocity of 1mm/sec was applied to compress the edge of the cylindrical shell in the analysis.

4. Numerical Examples

4.1 Eigenvalue Analysis

We carried out some analysis work in order to trace the findings by Yamaki et al., as summarized in Fig.3. The analysis model is shown in Fig.7. The object of the analysis is a model with Z=500. This model was fully constrained at its top and bottom ends and then compressed in the axial direction. As it is assumed some asymmetric deformation patterns are likely to occur, the entire body of the cylinder was modeled. Since any buckling mode could conceivably be sensitive to initial imperfections, all numerical data for the coordinates were carefully determined to maintain consistency in precision, so that an ideal geometry of the cylindrical shape could be generated. The model was divided into 24 meshes in the axial direction and 200 meshes circumferentially. The shell element S4R implemented in Abaqus is used for the analysis. As this element has a great advantage such that it can be used to model both of thin shell and thick shell structures for the strain-concerned applications, this element is currently widely spread to use for the industrial application problems. The reduced integration scheme helps in reducing the amount of CPU time, and also provides much accurate results than other schemes. It was fortune for us that no difficulty in numerical convergence due to possible hourglass behavior in this reduced integration element was met during the whole analysis process. We have confirmed that the fully integrated shell element S4 also gives a comparable result to S4R. For a medium length cylinder, the critical buckling mode involves square waves, and can be described in terms of the number of full waves along the circumference in this mode, given by

$$n_{cl} = \sqrt[4]{(3/4)(1-\nu^2)}\sqrt{r/t} \simeq 0.909\sqrt{r/t} \qquad \cdots (3)$$

For the analysis condition in this study, n_{cl}=18 was assigned. As shown previously, it is known from the current finding that many buckling modes exist simultaneously, and accordingly, Eq.(3) is of little significance [1]. However, determining mesh division, predicting the result from the eigenvalue analysis using this type of simplified formula is evaluated to be basic manner in order to carry out rational analysis. Totally more than 100 buckling modes were extracted within a range of 1.02～1.07 of the classical elastic critical stress. The extracted buckling stresses are slightly higher than the theoretical stress, because the length of the analysis model is finite. Some typical modes were selected among these modes and applied as the initial imperfection.

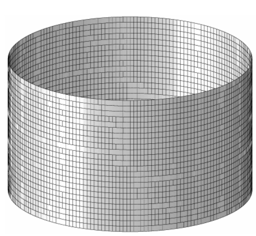

$$Z = 500\ \left(r = 100\text{ mm},\ t = 0.247\text{ mm},\ L = 113.9\text{ mm}\right)$$

$$E = 5560\text{ MPa},\ \ \nu = 0.3$$

$$\sigma_{cl} = \frac{E}{\sqrt{3\left(1-\nu^2\right)}}\frac{t}{r} = 8.31\text{ MPa}$$

$$P_{cl} = 2\pi rt \cdot \sigma_{cl} = 1290\text{ N}$$

Figure 7. Analysis model for Yamaki's cylindrical shell .

n=3 n=6 n=9 n=12 n=15

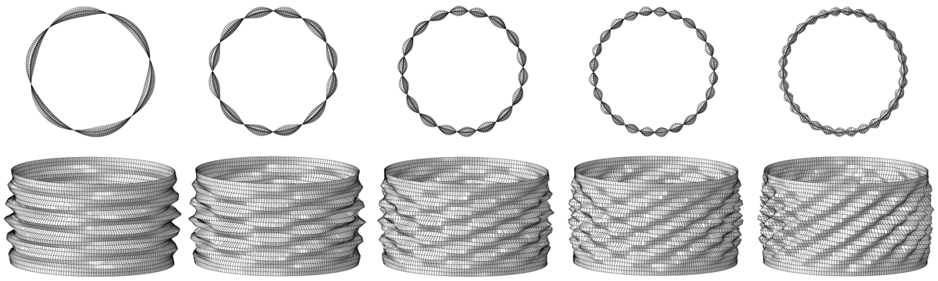

σ / σ_{cl} = 1.035 1.039 1.046 1.058 1.071

Figure 8. Results from eigenvalue analysis.

4.2 Arc-length Method

For the post-buckling analysis, the results using the arc-length method is first shown. The arc-length method implemented in Abaqus is well recognized by the author as being so much tough for 3D problems compared with other similar software. However, even using such a tough tool on this task only could give the level of solution as high as the results shown in Fig. 9, which is recognized as the limit of its capability. This study case was set up by imitating the achievement done by Teng and Hong [7] as shown in Fig. 4, that is to say, a single buckling mode (In Fig.9, it corresponds to the buckling mode with n=13) was assigned to the initial imperfection. As noted in the figure, point, A is distinguished as pre-buckling at which some slightly out-of-plane deformation is observed over the surface of the cylindrical shell, and point, B indicates the primary buckling which is the limit point with the deformation mode of n=13. The load at the primary buckling is somewhat lower than the classical critical load P_{cl} with the effect of the geometric nonlinearity. So far as the load path reaches to this region, deformation is spread over all the surface of the cylindrical shell, and accordingly this type of deformation can be straightforwardly analyzed using the arc-length method.

Whilst, after entering the post-buckling region, a single dimple (point, C) was produced locally on the surface of the cylindrical shell. As this behavior is known to be highly local deformation, use of the arc-length method may not be appropriate for solving such a deformation type. Such the mode having a single dimple is eventually led to the point, D of the secondary buckling. By further pursuing the deformation patterns, the analysis could find subsequent occurrence of further higher order of buckling modes associated with increasing the number of dimples one by one base as shown in point, E and point, F in Fig.9. The load at point, F was about 800N. If the solution by the arc-length method did not diverge, the number of dimples should have increased until filling the periphery of the cylindrical shell (up to n=13), and the analysis might be able to be progressed to find the minimal value on the load path. As described later, when the artificial damping analysis or the explicit dynamic analysis was used, we could find a unique manner in the load path such as the deformation mode directly jumped from the primary buckling point, B to this minimal value for n=13. As shown in Fig.10 later, the minimal value of the load at his jump was about 400N. Since, even in the actual behavior of such a structure, dynamic jumping of the deformation mode may occur, we may have no other choice than relying on the arc-length method in order to find every individual bifurcation path. But, besides the above, in the region immediately after primary buckling, as often mentioned before, there are many bifurcation paths. And it is easy to guess such that the other cases under the initial imperfection with the modes other than n=13 may behave differently to yield other solutions (i.e., different from the results in Fig.9). We would argue such that it would be so difficult for the current level of the analysis capabilities to derive general conclusion for 3D local buckling problems from the results obtained with use of the arc-length method.

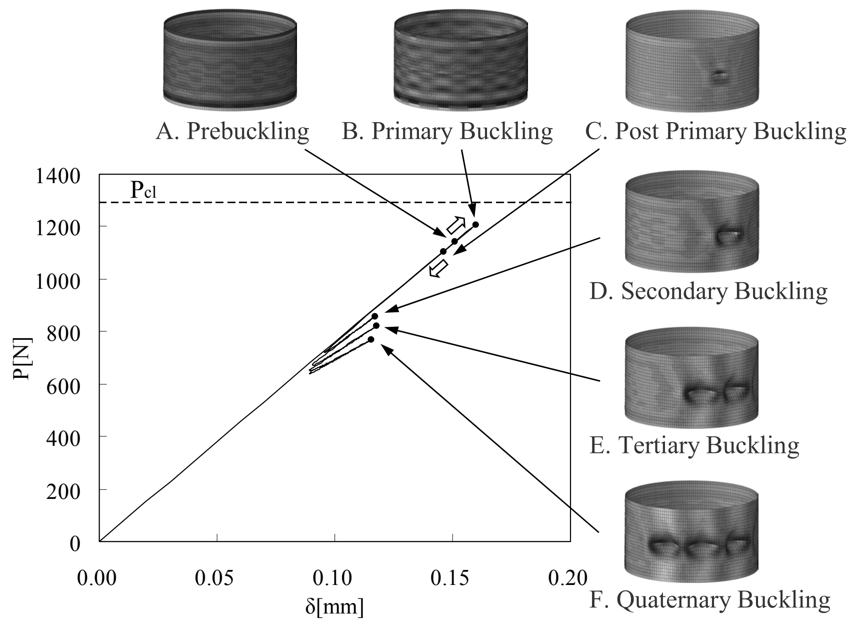

Figure 9. Results from arc-length method.

4.3 Artificial Damping Analysis and Explicit Dynamic Analysis

Abaqus enables us to achieve stabilization of the analysis with local instability using the artificial damping method. The results are shown in Fig.10. We can see a process of buckling point shifts in the manner of repeating of snap through from one curve to the next curve while the number of waves is decreasing in order of n=13, 12, 11, 10, and 9. The measured values in the experiments carried out by Yamaki et al. are also shown in Fig.10 by superimposing them onto the results from our FEM analysis. The results from the FEM analysis are found to almost overlap the measured values. In addition, as it can be seen in the figure, the use of the explicit method gave comparable solutions. According to the experimental results found by Yamaki et al., the number of the buckling waves initiated with n=12. The amplitude of the initial imperfection assigned to the analysis was 1/100 of the shell thickness, and the degree of the accuracy in the circle geometry of the cross-section is sufficiently high. Keeping such the level of the model may have led to finding of higher number of the waves than those found in their experiment. Note that the linear buckling mode used for the initial imperfection is composed with combining buckling modes up to n=15. As mentioned before, this initial imperfection works only as a trigger for initiating bifurcation, which produced results within a narrow range whatever assigned the mode provided with the buckling modes along the number of waves n=12 or more as observed in the experiment. Fig. 10 shows the analysis results including deep postbuckling region where the deformation largely grows. Viewing the overall postbuckling paths, local instability appears within the primary buckling region with simultaneously a big drop down of the load, and in the region after the secondary buckling, unstable progress of the deformation covering a wide range accompanied with mode jumping is observed. Overcoming such complicated process in the deformation, the whole range of the postbuckling paths could be analyzed employing the full auto-increment calculation.

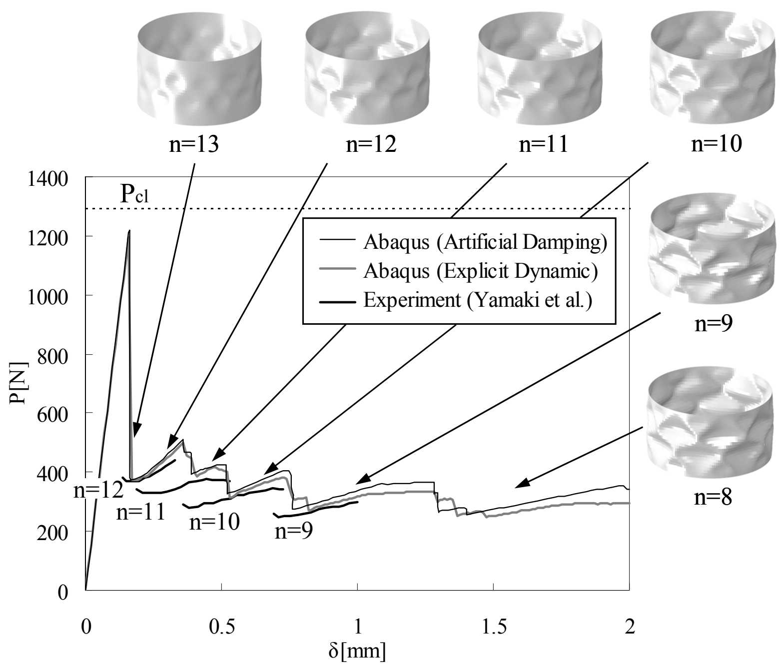

Figure 10. Results from artificial damping analysis and explicit dynamic analysis.

5. Conclusions

The analysis capabilities provided with the recent general-purpose FEM codes are regarded as being sufficiently enough to solve the highly nonlinear problems. By such enhancement, many engineers will be released from the burden of developing sophisticated programs – it's a great merit. In this study, a problem of cylindrical shells of perfect geometrical dimensions subject to axial compression is targeted. This is regarded as one of the most difficult tasks involved with buckling phenomenon. Based on the finding obtained from the previous research works, analysis policies to apply the nonlinear FEM capabilities are formulated and are implemented so as to be available in practical designs. It is successfully demonstrated that automatic streamlined analysis using both of the static analysis and the explicit dynamic analysis can be accomplished in a stable process well covering deep postbuckling region.

6. Acknowledgement

The authors wish to express his appreciation to Prof. Hirohisa Noguchi, Keio University, who gave many valuable suggestions and provided guidance from the view point of applicability of snap-through jumps between buckling modes with different numbers of waves and the effective use of the artificial damping method. However, it is with great regret to inform you that we received the sad news of the death of Prof. Hirohisa Noguchi in August, 2008. His memory will remain with us all.

7. References

1. Teng, J. G., and Rotter, J. M., "Buckling of Thin Metal Shells," Spon Press, p.2, pp. 42-72, UK, 2004.
2. Koiter, W. T., "On the Stability of Elastic Equilibrium," PhD Thesis, Delft University, 1945, English Translation in NASA TT F-10, 833, 1967.
3. Calladine, C. R., "Theory of Shell Structures," Cambridge University Press, UK, 1983.
4. Karman, T. H., and Tsien, H. S., "The Buckling of Thin Cylindrical Shells under Axial Compression," Journal of the Aeronautical Science, vol.8, p.303, 1941.
5. Donnell, L. H., and Wan, C. C., "Effect of Imperfections on Buckling of Thin Cylinders and Columns under Axial Compression," Journal of Applied Mechanics, vol.17, pp.73-83, 1950.
6. Yamaki, N., "Elastic Stability of Circular Cylindrical Shells," North-Holland, Netherlands, 1984.
7. Teng, J. G., and Hong, T., "Postbuckling Analysis of Elastic Shells of Revolution considering mode switching and interaction," International Journal of Solid and Structures, vol.43, pp.551-568, 2006.
8. Hong, T., and Teng, J. G., "Imperfection Sensitivity and Postbuckling Analysis of Elastic Shells of Revolution," Thin-Walled Structures, vol.46, pp.1338-1350, 2008.
9. Fujii, F., Noguchi, H., and Ramm, E., "Static Path Jumping to Attain Postbuckling Equilibria of a Compressed Circular Cylinder," Computational Mechanics, vol.26 (3), pp.259-266, 2000.
10. Sosa, E. M., Godoy, L. A., and Croll, J. G. A., "Computation of Lower-Bound Elastic Buckling Loads Using General-Purpose Finite Element Codes," Computers and Structures, vol.84, pp.1934-1945, 2006.
11. Abaqus Users Manual, Version 6.8, Dassault Systems Simulia Corp., USA, 2008.
12. ENV 1993-1-6, Eurocode 3: Design of Steel Structures, Part 1.6: General Rules-Supplementary Rules for the Strength and Stability of Shell Structures, CEN, Brussels, 1999.
13. Liu, W. K., and Lam, D., "Numerical Analysis of Diamond Buckles," Finite Elements in Analysis and Design, vol.4, pp.291-302, 1989.
14. Edlund, L., O., "Buckling of Metal Shell: Buckling and Postbuckling Behavior of Isotropic Shells, Especially Cylinders," Structural Control and Health Monitoring, vol.14, pp.693-713, 2007.